

Proposal 0132 & 0132A

See Proposal 154

Scientific Spokesman

Irwin A. Pless  
Laboratory for Nuclear Science  
575 Technology Square, Rm. 408  
Massachusetts Institute of  
Technology  
Cambridge, Massachusetts 02139

FTS/Commercial: 617-876-6073

A GENERAL SURVEY OF PION-PROTON AND PROTON-PROTON  
COLLISIONS IN THE 100-500 GeV/C REGION

D. G. Fong, A. M. Shapiro, M. Widgoff  
Brown University

G. Ascoli, B. Eisenstein, L. Eisenstein, J. D. Hansen, U. Kruse, R. Sard  
University of Illinois

R. A. Burnstein, L. Fu, H. A. Rubin, V. R. Veirs  
Illinois Institute of Technology

E. D. Alyea, K. F. Galloway, H. J. Martin, J. E. Mott, R. E. Mercer  
Indiana University

A. Pevsner, C. Chien, D. Denegri, R. A. Zdanis  
Johns Hopkins University

B. T. Feld, B. Haber, R. Hulsizer, V. Kistiakowsky, I. A. Pless,  
F. Triantis, J. Wolfson, R. K. Yamamoto  
Massachusetts Institute of Technology

N. N. Biswas, N. M. Cason, V. P. Kenney, W. D. Shephard, D. W. Thomas  
Notre Dame University

R. J. Plano, T. L. Watts, P. Yamin, A. Sheng, D. Pandoulas--E. Brucker,  
E. L. Koller, S. Taylor  
Rutgers University--Stevens Institute

H. Kraybill, H. Taft, T. Ludlam--D. Bogert  
Yale University--National Accelerator Laboratory

April 15, 1971

A GENERAL SURVEY OF PION-PROTON AND PROTON-PROTON COLLISIONS  
IN THE 100-500 GeV/c REGION

Submitted by:

Brown University, University of Illinois, Illinois Institute of Technology,  
Indiana University, Johns Hopkins University, Massachusetts Institute of  
Technology, University of Notre Dame, Rutgers University--Stevens  
University, Yale University--National Accelerator Laboratory.

15 April 1971

TABLE OF CONTENTS	PAGE
I. Cover Page - Title and Abstract	
II. Physics Justification	
A. Introduction	4
B. Particle Number and Distributions	8
C. Single Particle cross sections and Distributions	9
D. Diffraction Dissociation of Target	10
E. Diffraction Dissociation of the Projectile	13
F. Elastic Scattering and Total Cross Sections	14
G. Cross Section for $\pi^+ p$ Going to all Neutrals	16
H. Quasi-Two Body Production	17
I. Other Processes	18
J. Specific Tests of High Energy Theoretical Models	19
III. Beam Requirements	23
IV. Experimental Arrangement	
A. Equipment and Set Up	24
B. Data Analysis	25
V. Construction and University Testing Time	28
VI. Installation and Maintenance	29
VII. Costs	30
VIII. Finances and Management	31
IX. Summary	
References	36
Appendix I - Momentum Measurement	37
Appendix II - Particle Counting	40
Appendix III - Three constraint fits	42
Appendix IV - Measurement of Invariant Mass	47

## I. COVER PAGE

### TITLE AND ABSTRACT

#### A General Survey of Pion-Proton and Proton-Proton Collisions in the 100-500 GeV/c Region

The proposed experiment will provide an extensive, energy-dependent, rapidly analyzable early look at the general behavior of high energy hadron interactions in the 100-500 GeV/c region.

The experiment utilizes a hybrid system consisting of the 30-inch hydrogen bubble chamber and proportional chambers.

Experiments to date, including cosmic ray and accelerator research, have generated theoretical concepts which underscore the importance of the study of particle production in all reactions, with detailed attention to regular variations with energy and with the nature of the projectile and target. The proposed experiment will extend these kinds of studies through the range of energies available at NAL, with good event acceptance and moderate resolution. In addition the experiment will allow examination of coherent processes (elastic scattering and diffraction dissociation) which appear to give the only significant individual channel cross sections at very high energies.

A general survey with the bubble chamber is, of course, well suited to detect new phenomena which may arise from unsuspected sources in this relatively uncharted energy domain.

The use of proportional chambers external to the bubble chamber will ensure 1) spatial resolution of very forward secondaries (track counting) and 2) momentum information on all outgoing tracks up to 500 GeV/c. We expect an average of about eight beam tracks per machine pulse in a spill time of ~60 micro seconds. This high instantaneous data rate necessitates the use of proportional chambers.

This hybrid configuration will allow measurement of total cross sections (to a few percent), charged particle and topological cross sections, single particle momentum distributions, and particle correlations--including resonance production. In addition we will be able to study cross sections for the important phenomena of coherent production; the experiment holds promise of allowing complete analysis of individual events in these channels.

We require nine exposures equally divided among incident protons and positive and negative pions. Pictures will be taken at three different momenta spaced between  $\sim 100$  GeV/c and the highest available momentum. In order to test Quark Model predictions relating  $\pi p$  and  $pp$  cross sections we require one of the pion momenta to be  $\frac{2}{3}$  the highest proton momentum. A total of 2 million pictures is requested, resulting in  $\sim 55,000$  events for each of the 6 pion exposures and  $\sim 80,000$  events for each of the 3 proton exposures.

Each exposure will be analyzed independently by one or more of the participating groups, thus allowing a large amount of the analyses (covering a wide range of physics) to be carried out in parallel. This will enable a survey of much of the physics in this energy domain in a minimal amount of time. All participating groups will agree on the general method of analyses and agree on a common set of parameters to be used, i. e. fiducial volume, resonance shapes, optical parameters, etc. This general agreement among the participants will ensure consistent systematic errors and will therefore allow for meaningful energy and charge dependent studies.

The results of some of the simpler analyses would be completed within 6 months after data acquisition and the more complicated analyses would require about a year to complete.

Universities and Names of Experimentors:

High Energy P-P-	Massachusetts Institute of Technology
Medium Energy P-P-	Illinois Institute of Technology
Low Energy P-P-	Yale University — National Accelerator Laboratory
High Energy $\pi^-$ -P-	Rutgers University — Stevens Institute
Medium Energy $\pi^-$ -P-	Johns Hopkins University
Low Energy $\pi^-$ -P-	University of Illinois
High Energy $\pi^+$ -P	Brown University
Medium Energy $\pi^+$ -P	Indiana University
Low Energy $\pi^+$ -P	Notre Dame University
Spokesman:	Irwin A. Pless
Date:	April 29, 1971

## II. PHYSICS JUSTIFICATION

### A. Introduction

Experiments at these (100-500 GeV) high energies present unique experimental problems, and there is little experience to build upon. However, we have the empirical fact that the transverse momentum of individual particles in high energy collisions, independent of type of incident particle, momentum, or type of target has an average of 300 MeV/c. This fact makes it seem desirable to combine a modest size bubble chamber with a down stream spectrometer since this arrangement holds promise to allow the complete analysis of individual events. As is well known, this complete analysis has been fruitful in the energy region below 30 GeV and it seems likely that such an analysis will be useful in the 500 GeV region.

Ultimately, a high precision, magnetic spectrometer may be desirable for this type of investigations, and this proposal, should be viewed in part, as a first step toward this goal. The information gained from this experiment would allow us to design a more ambitious and useful spectrometer than the one contained in this proposal. We are proposing to use only the bubble chamber, and proportional chambers in this first experiment. We use the fringe field of the bubble chamber and the proportional chambers as extensions of the bubble chamber itself. This allows a far more precise measurement of the fast out going particles than can be achieved using the bubble chamber alone.



In fact, as will be described in the experimental arrangement and the appendices, the proposed arrangement is powerful enough to measure elastic scattering, do three constraint fits in the special case that the incident particle may suffer a small loss in energy, and measure invariant masses of highly energetic ( $\sim 100\text{GeV}$ ) charged particle configurations to the 10 per cent level. This will allow a tentative search for high mass resonances that decay into charged pions. In addition, one will be able to count higher charge multiplicities than can be achieved in a bubble chamber alone.

The above information exceeds what is achievable with a bubble chamber alone.

The use of proportional chambers are required to make the studies described below. The reasons are as follows:

1. Rapid cycling time.

It is necessary, to tag information, beam particle by beam particle. With each beam particle, one must associate the outgoing tracks. This is required both as a picture by picture calibration, as will be discussed later, but also to associate multiple particle events, without confusion, with a particular beam particle. Crucial to all analyses is the angle and momentum of the incident particle initiating an event. In addition, for the  $\pi^+$  exposures in particular, one will need Cerenkov information to identify the incident particle. Because of the cycling time, the proportional chambers need no trigger. All the information associated with each beam track will be stored separately in shift registers. Hence, there will be no trigger logic biases and no false triggers due to interactions in various walls or stray particles.

The strong point that we are making here is that a proportional chamber system will be free of the uncertainties associated with trigger logic. In addition, since the instantaneous data rate is exceedingly high (about one megacycle maximum) proportional chambers are the only choice.

## 2. Multiple particle efficiency.

It is required to measure an average of 10 particles (an extreme of 20 particles). Again, the most reliable device for this is the proportional chamber.

Using the power of the above system, there are several phenomenological models whose general predictions can be investigated. These are predictions about diffraction dissociation, limiting fragmentation, elastic scattering and total cross sections.

The incident particles would be proton and  $\pi^\pm$  mesons. The detection apparatus would be the small bubble chamber preceded and followed by proportional chambers mentioned above.

The beam spill should have three short pulses containing an average of eight particles which will be used for the bubble chamber in the triple pulse mode.

The experiment requires  $2 \times 10^6$  exposures equally divided between incident protons, negative pions, and positive pions. Each type of particle will be studied at three momenta - low, medium and high. Since the  $\pi^+$  beams may have as much as a 50% contamination, additional pictures (up to a factor of two) may be required for these exposures.

The universities listed in Section I agree to use a common fiducial volume and similar analysis techniques. The groups will endeavor, (as much as possible),

to ensure that meaningful energy dependent and charge dependent comparisons can be made. This is an extremely important aspect of the proposal. Only if there is a serious effort to control the experimental systematics in a uniform way will meaningful energy and charge dependent comparisons be possible. Since the members of this group are well aware of the inherent difficulties, they will take particular pains to minimize the problem.

## B. Particle Number and Distributions

There is, currently, considerable interest in the average number of particles produced in high energy collisions as a function of bombarding momentum. In addition, the charged prong distribution for a fixed projectile momentum is also of current interest. Our experimental setup will allow us to count accurately up to 20 charged particles. Since we expect an average of about 7 to 10 particles, we will be able to make an excellent measurement of the above quantities. Appendix II gives the details of our techniques for constructing tracks from the proportional chamber information.

We are able to resolve essentially all ambiguities because of the following facts:

1. We have an excellent measurement of the vertex of the event
2. Each proportional chamber consists of three planes placed at relative angles of  $120^\circ$  between them.
3. We have three chambers which allow a fit to a straight line.

The prediction of some models with respect to these quantities are discussed in section J.

### C. Single Particle Cross Sections and Distributions

As demonstrated in Appendix I we can make moderately accurate measurements on all outgoing charged particles. There is a smooth transition from measurements made in the bubble chamber alone to measurements made with the aid of the proportional planes. This transition comes at about 15 GeV/c where  $\Delta p/p$  is less than 10%.

This momentum accuracy on individual particles will allow a measurement of the longitudinal momentum distribution in the center of mass. In addition one can measure  $\frac{d^2\sigma}{dp_{||} dp_{\perp}^2}$ . Many theories (i. e. Yang, Feynman, etc.) make specific predictions about these quantities.

The type of process one studies here is known as "inclusive reactions". The prediction of various models with respect to these inclusive reactions is discussed in section J.

### D. Diffraction Dissociation of Target

There seems to be no accepted definition for diffraction dissociation processes. In fact, a definitive description does not exist for any diffractive process. The following seem to be agreed on as general properties of diffraction dissociation.

1. The cross sections for such processes vary slowly with increasing bombarding energy.
2. No exchange of isotopic spin quantum numbers, strangeness and baryon number takes place.
3. The diffraction dissociated system is characterized by a low invariant mass.
4. The process occurs at small momentum transfers.
5. No G-parity exchange takes place.

The above properties are sometimes described as a Pommeranchuk exchange or a vacuum exchange. Such processes were first discussed explicitly (and named) by Good and Walker<sup>(1)</sup> in 1960. Since then they have been discussed by other authors, in particular, Yang<sup>(2)</sup>. Yang characterizes these processes as those in which the target breaks up into  $n$  particles such that the total  $G$ ,  $I^2$ ,  $I_z$  and charge of these  $n$  particles equals that of the target.

Jackson<sup>(3)</sup> discusses the Pommeranchuk or vacuum trajectory as something special in the "hierarchy of Regge poles because (i) it is the highest lying trajectory, (ii) its slope seems abnormally small ( $\alpha'_p \approx 0 - 0.3 \text{ (GeV/c)}^2$ ), and (iii) there are serious doubts that it is a simple Regge pole. Some of the doubts concern the apparent slope and the lack of particles to associate with this trajectory; others

stem from a belief that diffractive scattering is a complicated shadowing effect, far more involved than the exchange of a single Regge pole."

The reactions that this experiment will explore are:

$$P+P \rightarrow P+(P\pi^+\pi^-) \quad - \quad (1)$$

$$P+P \rightarrow P+(P\pi^+\pi^-\pi^+\pi^-) \quad - \quad (2)$$

$$\pi^\pm+P \rightarrow \pi^\pm+(P\pi^+\pi^-) \quad - \quad (3)$$

$$\pi^\pm+P \rightarrow \pi^\pm+(P\pi^\pm\pi^-\pi^+\pi^-) \quad - \quad (4)$$

In the notation of Yang<sup>(2)</sup> the bracketed quantities form a  $P^\dagger$ . In these reactions the projectile (either proton or  $\pi$ ) loses very little energy and leaves behind the  $P^\dagger$ . The prediction of Yang's theory is that these cross sections should remain constant or vary slowly with increasing energy of the projectile. Most of the other theories also imply a constant cross section as a function of energy for the above reactions. In particular, at high energies one expects that each of the above reactions will have a cross section which is a constant fraction of the elastic cross section.

In Appendix III we demonstrate that we can separate out the above reactions from the case when an additional  $\pi^0$  is produced, we expect to measure the cross section for this reaction and the  $t$ -dependence as a function of the mass of the  $P^\dagger$ . There are experimental data on reactions (1) and (2)<sup>(5)</sup>. If these cross sections have reached their limiting value at 30 GeV/c, then we can expect a constant cross section of 1.0 mb out to 500 GeV/c. However, if the indicated general downward trend continues, we can expect a cross section of about 0.03 mb. This experiment can easily tell the difference between these extremes.

There is little experimental data on reactions (3) and (4). Since the  $\pi P$  elastic scattering cross section is approximately half that for  $PP$  elastic scattering, one

would expect reactions (3) and (4) to have about half the cross sections of reactions (1) and (2). If these reactions are indeed related to a Pomcranchuk exchange, then one would also expect the corresponding channels to have the same properties regardless of whether or not a proton or pion initiated the event.

Various models make predictions about this "exclusive reaction", and this is discussed in section J .



### E. Diffraction Dissociation of the Projectile

If the projectile is a pion and it diffractively dissociates into three charged pions, we will be able to measure the mass of the three pion system. This is shown in Appendix IV. Again, the energy dependence of this "exclusive" process is of current interest. If one considers this to be an example of Pomeron exchange this cross section should be a constant function of energy. This could be an efficient technique for locating high mass Bosons that are diffractively produced.

## F. Elastic Scattering and Total Cross Sections

The measurement of the elastic differential cross sections near  $t = 0$ , as a function of beam energy, will determine the slope parameter  $b$  for  $\frac{d\sigma}{dt} = \left. \frac{d\sigma}{dt} \right|_{t=0} e^{bt}$ . The dependence of  $b$  on laboratory momentum will shed some light on the slope of the Pomeranchuk trajectory. In particular, it would be of interest to see if  $b$  continues to "shrink" for PP scattering at energies greater than 100 GeV. A parameterization of this shrinkage, which includes the Serpukhov data is given by

$$b = b_0 + 2b_1 \ln \frac{S}{S_0}$$

where  $S_0 = 1 \text{ GeV}^2$ ,  $b_1 = .47 \pm 0.9 \text{ GeV}^{-2}$ ,  $b_0 = 6.8 \pm 0.09 \text{ GeV}^{-2}$ . Considering the situation at 500 GeV/c, then, this would predict a slope of  $b = 12.6 \text{ GeV}^{-2}$ .

Assuming this value and that the elastic and total cross sections stay constant from their values at 30 GeV/c, then we would expect to have 80,000 PP interactions of which 20,000 would be elastic events. There would therefore be over 10,000 events with  $|t| \geq 0.05 (\text{GeV}/c)^2$  which is the region where we expect to be able to resolve the elastic events with very good efficiency (see Appendix III).

With these statistics we expect to be able to measure this slope to better than  $\pm 0.15 (\text{GeV}/c)^2$  which represents a  $1 \frac{1}{2} \%$  measurement. This accuracy will allow the determination of shrinkage.

For the  $\pi^\pm$  beams, we expect 55,000 events which should contain 10-12,000 elastic interactions.

If we assume an  $e^{-7t}$  distribution for these elastic events, then there are over 8500 events which can be separated. This will allow an accurate determination of whether there is any shrinkage present at these energies. This is important to determine since there has been no evidence of shrinkage up to 30 GeV/c.

The measurements of  $\pi^\pm$  total cross sections, which can be carried out in this experiment to about 0.5 - 1.0% statistical error, will be valuable for checking the Pomieranchuk theorem. The  $\pi^\pm$  cross sections up to  $\sim 30$  GeV/c seem to be approaching a common constant value ( $\sim 21$  mb), as predicted by the Pomieranchuk theorem. However, at energies above 30 GeV (measured at Serpukhov), the implications are that the cross sections are fixed at their respective 30 GeV values (24.5, 23.5 mb), thus separated by  $\sim 1$  mb. Thus, measurements of these cross sections near and above Serpukhov energies would be an interesting check of the Pomieranchuk theorem.

In addition, we can measure the total elastic cross section, correcting in the usual way, for the loss of events at very small  $t$ . The energy dependence of these total elastic cross sections is of current interest.

### G. Cross Section for $\pi^- + p$ going to all Neutrals

The cross section for the reaction

$$\pi^- p \rightarrow \text{neutrals}$$

has been studied at low momenta where it decreases with increasing momentum.

The behavior of this cross section at high momenta would be readily obtainable from our experiment since the events would be tagged by a good incoming particle trigger without an accompanying outgoing particle trigger.

## H. Quasi-Two Body Production

The existence of two body or quasi two body reactions can be investigated. In general, if such reactions result from the exchange of any known particles [or Regge trajectories, excepting the Pommeranchuk], the individual cross sections are expected to fall off rapidly, as some power of the incident momentum. Nevertheless, it will be interesting to look for evidences of these reactions, especially of those reactions that might contain new resonances of higher mass than those already known that decay into charged mesons.

## I. Other Processes

It would be of interest to look for final states that are not expected to occur due to violation of present theoretical concepts or empirical observations. These would be, for example, processes that can occur only by so called "exotic" exchanges, viz. a doubly charged exchange,  $Z^*$  ( $s = 1$  baryon) production, etc.

Reactions where pions are produced with very low momentum in the center of mass ("pionization") apparently have an appreciable cross section at about 30 BeV/c. However, there is confusion with the pions from the peripherally produced  $N^*$ 's. At higher momenta this ambiguity is removed and it would be interesting to determine whether pionization does or does not occur at higher energies. Yang speculates it does not.

If the average multiplicity  $\langle n \rangle = \ln S$  then in the language of the muliperipheral model, the energy of adjacent particles ( $S_{ij}$ ) should be a constant, independant of energy, with value  $\sim 600$  MeV. We will measure this quantity as a function of energy.

## J. Specific Tests of High Energy Theoretical Models

While the purpose of this experiment is largely to provide new data in a systematic way over the range of NAL energies, there are a number of specific theoretical concepts based on existing data which may be usefully confronted by the studies outlined above. In particular, the limiting fragmentation hypothesis of Yang and co-workers, the parton model of Feynman, Regge phenomenology and various versions of statistical, multiperipheral, and quark models. In many respects these ideas result in similar predictions.

Some specific tests are outlined below:

- 1.) Multiperipheral and scaling models (such as that of Feynman) predict a variation of average multiplicity of charged secondaries as

$$\bar{n} = a \ln S + b \quad (S = \text{square of C. M. energy})$$

whereas statistical models predict

$$\bar{n} \propto S^c, \quad c \approx \frac{1}{4}$$

Present data (Jones et al.) up to 680 GeV in cosmic ray studies do not distinguish between these alternatives.

- 2.) Implicit in multiperipheral models is a Poisson distribution in the number of charged secondaries. Similar, but not identical distributions are suggested by other theories. Present data are inconclusive in distinguishing between these possibilities, with some indication that such a distinction may be made with good data over a larger range of energies than those studied to date with accelerator data.

- 3.) Recent work by Chan et al. gives quantitative predictions relating single particle spectra to Regge behaved amplitudes.
- 4.) Using an additive quark model, Satz predicts one-to-one relationships between multipion final states from NN and  $\pi$ N reactions, provided the laboratory momenta at which cross sections are compared are in the ratio  $P_{\text{lab}}^N / P_{\text{lab}}^\pi = 3/2$ . With this in mind, we require that one of the pion momenta in the experiment be  $2/3$  the highest proton momentum.

Erwin et al. have observed in a 25 GeV  $\pi$ P experiment some evidence for this sort of behavior, viz. that the longitudinal momentum distributions of produced pions are symmetric in the Lorentz frame in which ratio of incident proton momentum to incident pion momentum is 3:2. It will be of great interest to examine this relationship at very high energies where the kinematic effects become less important.

- 5.) The limiting fragmentation model of Yang et al. <sup>(2)</sup> characterizes the product distribution in terms of limiting distributions of fragments resulting from the disruption of the target or the incident particle in question. From their point of view, diffraction dissociation is regarded as the special case where the projectile fragments and/or target fragments have the same quantum numbers as the projectile and target particle respectively. The preferred system to analyze the target break up is the laboratory system, while the preferred system to analyze the projectile break up is the rest frame of the incoming particle.

This limiting fragmentation distribution for a given product is characterized by a momentum density distribution,  $\rho_1(\vec{p}_1) d^3 p_1$ . According to Yang's approach this function approaches a limiting distribution at high energies. In this experiment, the slow particles in the bubble chamber should represent this limiting fragmentation of the target, whereas the fast forward-going particles should represent fragmentation of the projectile.



In particular, it is of interest to see whether  $\frac{\partial^2 \sigma}{\partial p_{||} \partial p_{\perp}^2}$  approaches a limiting distribution and whether this distribution is factorizable into functions of longitudinal and transverse momentum, i. e.,  $\frac{\partial^2 \sigma}{\partial p_{||} \partial p_{\perp}^2} = f(p_{||}) g(p_{\perp})$ . The form of  $\frac{\partial \sigma}{\partial p_{||}}$  is also interesting, i. e., is  $\frac{\partial \sigma}{\partial p_{||}} \sim p_{||}^{-1}$  as is expected from multiperipheral models? Present data at 25 and 30 GeV seem to indicate that this factorization is not obeyed.

Any resonance, e. g.,  $N^*$ ,  $\Delta^{++}$ ,  $\rho^0$ , etc., which has a small momentum in the laboratory can be measured, and so the behavior of these cross sections can be compared with the limiting fragmentation hypotheses as well as those for pions and protons.

Distinctions between the multiperipheral and fragmentation concepts may be explored by examining correlations between the transverse momenta of produced particles. That is, as suggested by Yang, the multiperipheral models require  $\langle \vec{p}_t^i \cdot \vec{p}_t^j \rangle < 0$ , where  $\vec{p}_t^i$  is the  $i$ th transverse momentum vector. No such correlation is required by the fragmentation hypothesis. Similar correlation tests have been suggested by Bjorken and others.

In the event of strange particle production, limiting fragmentation would imply the production of the strange meson in association with a hyperon fragmenting system. This can be investigated.

- 6.) Feynman<sup>(10)</sup> treats specific reactions as involving either exchange or radiation of a spectrum of "partons" characterized, in the limit of infinite c. m. momentum,  $W$ , by the distribution  $dx/x$ , where  $x = P_z/W$  is the center of mass longitudinal momentum of the product or products in question in units of  $W$ . In the Feynman approach,  $x$  and  $Q^2$ , the total transverse momentum, are the appropriate variables in terms of which a given set of reaction products should be analyzed.

Specific reactions are expected to exhibit Regge behavior i. e. , amplitudes proportional to  $s^{\alpha(t) - 1}$  where  $\alpha(t)$  corresponds to the leading Regge trajectory.

Among the various specific reactions, only those represented by Pommeranchuk exchange,  $\alpha(0) = 1$ , (elastic scattering, diffraction dissociation) are expected to survive in the asymptotic limit  $W \rightarrow \infty$ . However, the residue of various inelastic reactions (whose number go to infinity as  $W \rightarrow \infty$ ) should have a limiting single particle distribution in the center of mass that is proportional to  $dx/x$ . This  $dx/x$  particle distribution can be looked for in this bubble chamber experiment.

- 7.) Some Regge models make explicit predictions about the two particle inclusive process. This cross section can be written as:

$$\frac{2\pi}{\sigma_{ab}} \frac{d^5\sigma}{dP_{\perp}^2 dP_{\parallel} dP_{\perp}'^2 dP_{\parallel}' d\phi} = \frac{1}{\sigma_{ac}} \frac{d^2\sigma_{ac}^P}{dP_{\perp}^2 dP_{\parallel}} \times \frac{d^2\sigma_{bd}^{P'}}{\sigma_{bd} dP_{\perp}'^2 dP_{\parallel}'^2}$$

In the above  $P_{\perp}$ ,  $P_{\perp}'$ ,  $P_{\parallel}$ ,  $P_{\parallel}'$  are the transverse and longitudinal momentum of each particle while  $\phi$  is the angle between the two transverse momentum vectors.

In this experiment we will be able to test if the above cross section is independent of  $\phi$  and if the cross section factorizes.

### III BEAM REQUIREMENTS

The following beam specification and instrumentation are required for this experiment:

- 1) Unseparated secondary  $p, \pi^-$  beams and unseparated tertiary  $\pi^+$  beam, each at 3 different momenta between  $\sim 100$  GeV/c and the highest available momentum.
- 2) Three beam pulses per machine cycle with spills  $\sim 60 \mu s$  to fully utilize the triple-pulsing capability of the 30 inch bubble chamber.
- 3) Fast kicker-magnets with rise time  $\sim 1 \mu s$  to control the beam flux to  $\sim 8$  particles per bubble chamber pulse.
- 4) Seven proportional planes (a minimum of five planes plus two additional planes for redundancy checking) in the beam line upstream from the bubble chamber to supply the following beam data on a particle by particle basis:
  - a. beam entrance position at the bubble chamber within  $\pm 0.25$  mm.
  - b. beam angle with  $\Delta \theta = 0.02$  m rad.
  - c. beam momentum with  $\frac{\Delta p}{p} = \pm 0.05\%$
- 5) A threshold Cerenkov counter to work in conjunction with the proportional planes to supply mass tagging information of each beam particle which is vital to an unseparated  $\pi^+$  beam.
- 6) Access to an on-line computer with a magnetic tape unit to record frame number, magnet currents, Cerenkov counter output and readings from the upstream proportional planes and from those downstream which the experimenters in this proposal will supply. For a computer of  $\sim 2 \mu s$  cycle time,  $\sim 300$  ms of CPU time (integrated time) per machine cycle with  $\sim 4k - 5k$  (12 bit - 16 bit) words of memory will suffice to do this data logging.

#### IV. EXPERIMENTAL ARRANGEMENT

##### A. Equipment and Set Up

This experiment will require the use of a hybrid system consisting of a small bubble chamber, proportional chambers and scintillation counters. Figure 1 is a schematic of the set up. The incoming beam is defined by the scintillation telescope C and small proportional planes 1, 2. The fast, outgoing particles are analyzed by the proportional planes 3, 4, 5, 6 and 7. The geometry is chosen for incident particles of 500 GeV. The chamber sizes are 30 cm x 30 cm with 1 mm wire spacing. This implies 300 wires per proportional plane. Three planes with relative angle of  $120^\circ$  between them define each chamber, for a total of 900 wires.

The chamber closest to the bubble chamber will consist of pairs of planes displaced by  $\frac{1}{2}$  mm. This gives an effective  $\frac{1}{2}$  mm spacing for this plane. Doing this improves our momentum resolutions for the lower momentum by a factor two.

The scintillation telescope C will act as a trigger to read out all the wires of the proportional chambers into buffer store after each beam particle passes through the bubble chamber. The gathering of the data will be done with the aid of a small computer (PDP-11 class). All data will be recorded on magnetic tape. The computer will be used to spot check part of the experiment in real time, but the main data reduction will be off line. In addition, the particles that pass through the equipment without interacting will be used as a continual check on the alignment of the chambers. Since the incident beam will be well known, both in momentum and angle, picture by picture, interactions can be calibrated relative to non-interacting beam distributions.

## B. Data Analysis

In this section we show how we will make the measurement described in Section II.

### Particle Number and Distribution (IIB)

To study charged multiplicities, one has to have high efficiencies for multiple particles in a proportional chamber. Proportional chambers have this efficiency. In addition, one must be able to resolve the ambiguities inherent in this situation. Each proportional plane in this experiment is actually three planes, each at  $120^\circ$  to the other two. Appendix III demonstrates, again by Monte Carlo, that this setup resolves more than 99% of track ambiguities.

### Single Particle Cross Sections and Distributions (IIC)

To investigate this subject, it is necessary to measure single particle momentum with moderate accuracy. Appendix I demonstrates, again by Monte Carlo, that our "extended" bubble chamber allows about 5% accuracy on all particles up to 100GeV/c. This is accurate enough to explore the prediction in Section (IIC). Appendix I contains a curve exhibiting the momentum dependence of our accuracy.

### Diffraction Dissociation of Target (IID)

This process is very peripheral; therefore, the incident particle will experience a small deflection. Hence, this particle will traverse all 5 downstream chambers and an accurate path of its trajectory is known from the vertex to chamber 7. The diffracted system will consist of slower moving particles whose momentum can be measured with bubble chamber accuracies. This situation can be considered as a 3 constraint fit. In Appendix I, we display a Monte Carlo result of the comparison

of this three constraint situation with respect to the case where a pi-zero is produced with the charged pions. If the cross section for producing additional pi-zero's is equal to that of the systems described in (II D), we would expect a contamination in our 3 constraint sample of the order of 3%. Even if this contaminated cross section is 5 times larger than those in II D, the amount of contamination introduced in the sample would be at an acceptable 15% level.

#### Diffraction Dissociation of Projectile (II E)

In order for us to study this process, the projectile would have to decay into charged pions. In that case, we can make a reasonable measurement of the invariant mass. This is indicated in Appendix IV.

### Elastic Scattering and Total Cross Section (II F)

The fact that this equipment can distinguish elastic scattering from the situation where a pi-zero is produced is demonstrated in Appendix III. One has a 3 constraint fit which separates out the elastic scattering with a contamination of less than 1% for the region where  $t \geq 0.05$ . One recalls that the elastic scattering should be the dominant cross section. The proportional chambers will allow a measurement of the total cross section (0.5% - 1.0%). This is because one will have a beam particle by beam particle count of the flux and a "tag" for the difficult zero prong events. In addition, each picture will be electronically tagged for events, and there will be a pointer to the beam track that contains the event. Hence, the pictures will be electronically scanned for events, and the scanning personnel will only identify the type of event. The "scanning" biases should be small.

### Cross Section for $\pi^- + p$ Going to All Neutrals (II G)

As stated above candidates for this reaction will be tagged electronically and can be identified by scanners. The biases for this measurement should therefore be small.

### Quasi-two Body Production (II H)

Appendix IV indicates that we will be able to measure the invariant mass of a 100 GeV/c charged particle distribution to the order of 10%. If there is copious production of relatively narrow, heavy resonances we will be able to identify them.

### Other Processes (II I)

Appendix I indicates that the momentum measurements made on single particles will easily allow the study of "Pionization".

Appendix IV shows we can measure the invariant mass of a 500 MeV particle to 10%.

## V. CONSTRUCTION AND UNIVERSITY TESTING TIME

There are two major items [besides the bubble chamber] to consider. The first is the design, construction and testing of the proportional chambers. The second is the programming for the on-line data acquisition.

With respect to the proportional chambers, we intend to copy the NAL design exactly. It is our intent that the equipment we build will be completely compatible with all NAL equipment, including plugs and cables.

Again, the computer programs we write will be coordinated with the NAL staff so that our programs will be completely compatible with the NAL work.

The universities will be responsible for five chambers or 15 proportional planes. At the rate of 1 proportional plane per week, it will take 15 weeks to construct and test these five chambers. If the read out electronics is carried out in parallel, it is possible to be ready in four months with construction and university site testing. Using a contingency factor of two, it is possible to have tested equipment at NAL within eight months of start up time.

The on-line computer work should be similar to work we have already done in other experiments. University writing and testing can certainly be done in eight months.



## VI. INSTALLATION AND MAINTENANCE

Installing the equipment and maintaining it after it becomes operational is a major task. During the bubble chamber operation a full time crew, 24 hours a day and 7 days a week will be required. To recruit this group, for each exposure under section I, the responsible university will furnish one qualified person who will be available, at all times, to be present at NAL until this experiment is completed. This will be a nine man crew which will man the four shifts per week whenever the bubble chamber is operating. This same crew will be responsible for the initial installation.

If the bubble chamber is in operation before the upstream and downstream proportional chamber system is installed, it will be extremely useful to have pictures from the bare chamber. These pictures will be used to determine the optimum position of the downstream chambers. If the proportional chamber system is operational before the bubble chamber, it will extremely useful to get beam time to test the chambers. This test will be made with a small  $\text{CH}_2$  target and will allow us to test not only the chambers but also test some (but not all) of our off line programs.

## VII. COSTS

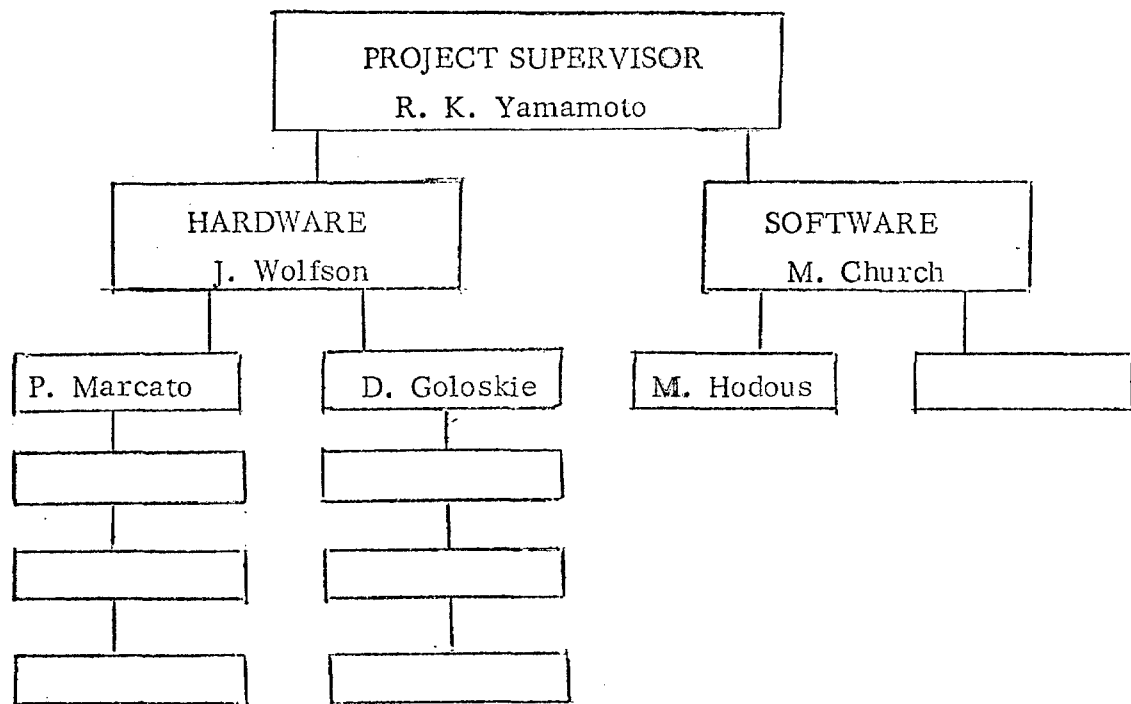
The following costs are based only on equipment. Labor will be furnished by existing people at the universities. This labor, in principle, could be the nine-man crew mentioned above. We assume no engineering costs, as we will follow the NAL design exactly. The total system we are discussing contains 5,400 wires. At \$10.00 per wire, this amounts of \$54,000. We need only a small amount of core and only a small amount of CPU time for our experiment. To be precise, we need 5,000 words of core and 300 milliseconds of CPU time per machine cycle. Either the universities will provide this computer or we could use one furnished by NAL.

### VIII. FINANCES AND MANAGEMENT

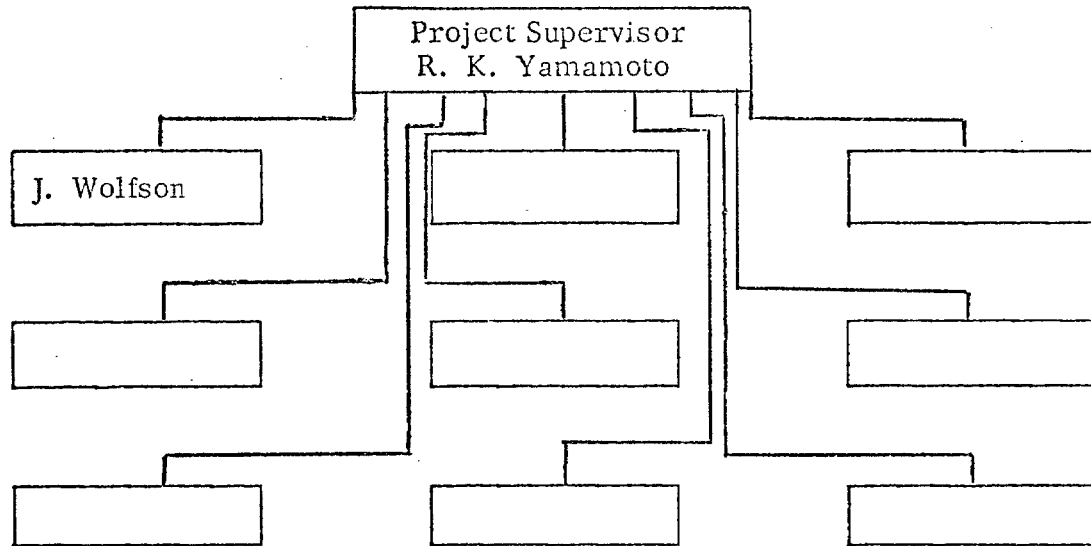
The funds for this experiment can come from three possible sources: Incremental funding from the AEC; allocation of funds from NAL; or from the universities. In particular, for each exposure under Section I, the responsible university is prepared, if funds are not otherwise available, to seriously approach its university administration with requests for \$15,000 to finance this experiment. This will furnish a basic budget of \$135,000.

The management of this project will be as follows:

A. Construction and Testing



B. Installation and Maintenance

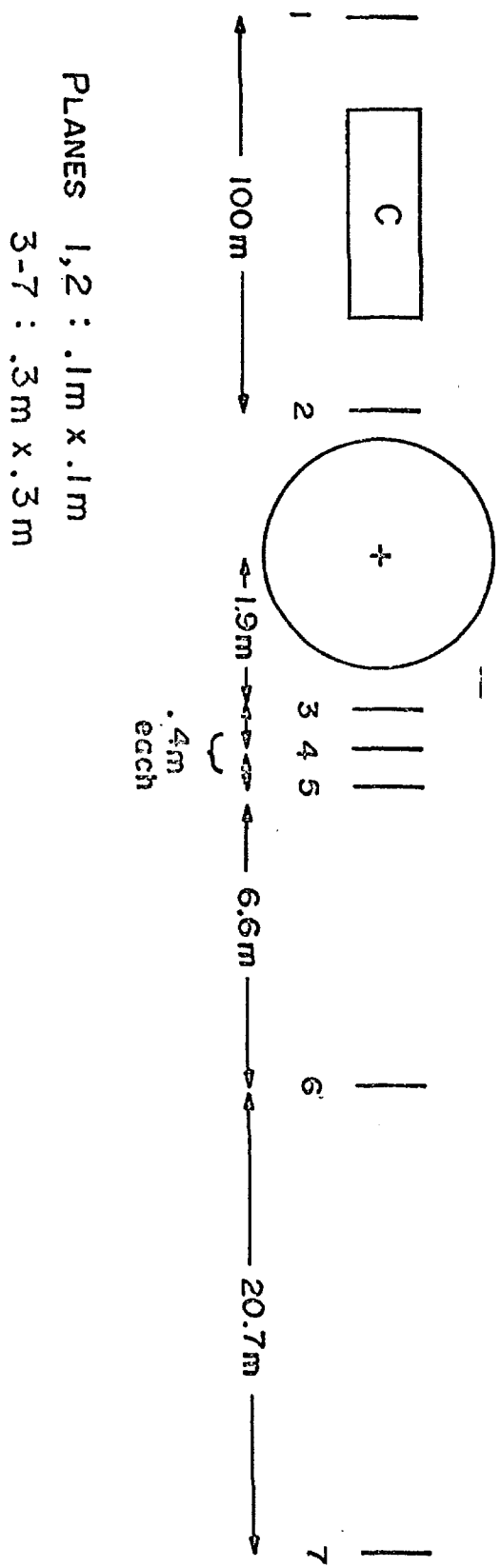


The above will obviously have to be carefully coordinated with the responsible people at NAL, and we will integrate our operation with NAL as closely as possible.

## IX. SUMMARY

We are proposing a comprehensive physics survey of the 100-500 GeV/c momentum range using incident proton, negative pions and positive pions on hydrogen. The experimental technique is the 30" Hydrogen Chamber followed by a simple set of proportional chambers. In addition, the experience gained by use of this simple downstream spectrometer will yield the necessary experience that will lead to the proper design of a more complex magnetic design incorporating the use of proportional chamber gamma ray detectors.

The universities will be responsible for the construction, installation and maintenance of these chambers for the duration of the experiment.



## REFERENCES

1. Good and Walker, Phys. Rev. 120, (1857) (1960).
2. J. Beneche, T. T. Chou, C. N. Yang, and E. Yen, Phys. Rev. 188 2159 (1969).
3. Proceedings of the Lund International Conference on Elementary Particles, 1969, page 80.
4. Proceedings of the Lund International Conference on Elementary Particles, 1969, page 174.
5. J. V. Allavy et al, Phys. Letters 28 B 67 (1968).
6. E. W. Anderson et. al, Phys. Rev. Letters 24 683 (1970).
7. C. B. Chiu and J. Finkelstein. Nuovo Cimento 57 A, 649; 59A, 92.
8. J. Orear, Physics Letters 13 (190) 1964.
9. Science Accessories Corporation, 65 Station Street, Southport Conn. This precision is stated to be  $1/4$  of a wire spacing. We have used in all our calculations  $1/2$  of a wire spacing.
10. Feynman, Phys. Rev. Letters 23 1415 (1969) and "Behavior of Hadron Collisions at Extreme Energies" Preprint October, 1969.



## APPENDIX I

## Momentum Measurement

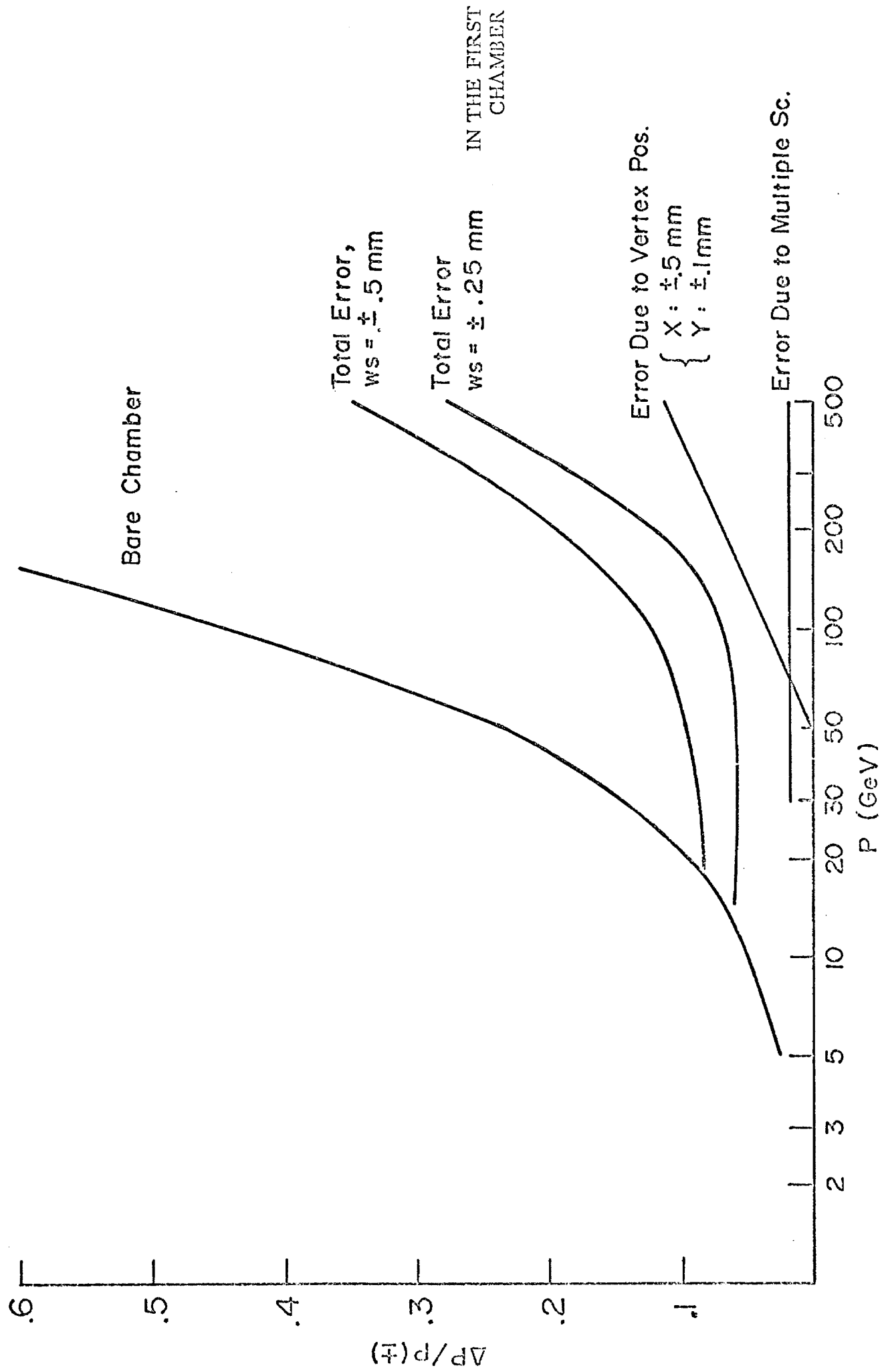
We have investigated the ability to measure the momentum of fast secondary particles from a high energy interaction using just the position of the vertex, the total magnetic field of the 30" HBC (including fringe field) and the final trajectory of the particle. The trajectory is determined by the array of proportional planes discussed in Appendix II. An additional fourth set of planes is located at a distance of 930 cm to give a better measurement of the angle for the very fast particles.

Several thousand Monte Carlo events were then thrown at various momenta from 10 to 500 GeV/c. At all momenta the particles were given a 300 MeV/c. transverse momentum with a gaussian width of  $\pm 100$  MeV/c. The particles were then swum through a magnetic field with the same length and the same integral of  $B \cdot dl$  as the 30" HBC magnet, although a constant value of B was used for ease of calculation. The various parameters were then given a random spread to simulate measuring errors by the following amounts.

1. The vertex position was perturbed by  $\pm 100 \mu\text{m}$  in the direction perpendicular to the beam and  $\pm 500 \mu\text{m}$  along the beam direction.
2. The particle's position as it left the magnetic field was perturbed by  $\pm 250 \mu\text{m}$  (1/2 of a wire spacing).
3. The angle of the particle as it left the field region was perturbed by  $\pm .5$  mr if it went through only the first three sets of planes and by  $\pm .05$  mr if it went through all four planes. This error was determined by taking the position errors in the planes ( $250 \mu\text{m}$  for the first plane and  $500 \mu\text{m}$  for the others) and dividing by the distance between the first and last planes traversed. It was also perturbed by an amount which corresponded to the multiple scattering of the particle in traversing half of the chamber and the exit windows of the chamber and vacuum tank.

The results of these calculations are shown in the figure on page 3 of this appendix. The bottom two curves show the contributions to the total error from the multiple scattering and the uncertainty in the vertex position. For wire spacing of 0.5 mm for the first plane and 1mm on all others, we get a total error which starts at  $\sim 5\%$  and rises to  $\sim 28\%$  at 500 GeV/c. Also shown are the errors if the wire spacing is 1mm for all planes and for the bare chamber.

It should be noted that by 20 GeV/c practically all of the particles are entering the downstream system while below 20 GeV/c the errors from measuring in the bare chamber are the same or better than those from the downstream system. There is, therefore, no 'hole' in our ability to measure fairly well the momentum of all particles from threshold to over 100 GeV/c.



## APPENDIX II

### Particle Counting

A Monte Carlo technique has been used to determine the ability of three sets of proportional planes to count and find the trajectories of the secondary particles from a high energy interaction. The following geometry for the proportional counters has been assumed.

Three sets of planes are located at 190, 227, and 264cm. from the center of the 30" HBC. Each set of planes consists of three square planes 30 cm on a side. Each plane contains 300 wires which are 1mm apart, and the three planes in each set are at an angle of  $120^\circ$  with respect to each other. The first chamber has a double set of planes giving in effect spacing of  $\frac{1}{2}$  mm.

With this geometry, then, a Monte Carlo was used to throw 10 prong events where all particles were constrained to come off at an angle of 60mr or less so that they traversed all three sets of planes. For each plane it was determined which wire would be fired by a given particle and the number of this wire was stored. If this particular wire had been fired by a previous particle in the same event, no additional entry was made into the table. Finally, then, there are 9 tables, one for each plane, each containing the numbers of up to 10 wires in that plane which have fired. Reconstruction is then done in the following way:

- a) For the three planes, which make up a single chamber, all possible hits are found by first finding (x, y) pair for all pairs of wires in the first two planes of a set. This (x, y) is then used to predict which wire in the third plane should have fired. If this wire ( $\neq 1$ ) has fired, then this particular (x, y) is stored as a possible hit.

b). The x coordinate of a hit in the first set of planes is then used to predict an x coordinate in the second set of planes -i. e. this is considered as the direction parallel to the magnetic field and therefore independent of momentum. If a hit at that coordinate is not found, the original (x, y) pair is rejected as spurious while if a hit is found, the two pair of (x, y) are used to predict an (x, y) in the third set of planes. If the third set is found then we consider that a real particle and its trajectory have been found. It should be noted that particles which hit the first two planes but miss the third can also be easily selected out while a particle which hits only the first plane must be coming off the vertex at a reasonably large angle and/or with low momentum and can be located from the film.

Using this technique, then, we have a spurious signal rate  $\cong .5\%$ . Most of this small spurious signal could probably be removed by a more detailed treatment of the problem. It has been assumed that the planes are 99.5% efficient.

An unavoidable problem in any hybrid system of this type is the production of high energy electrons by conversion of  $\gamma$ -rays in the exit window of the bubble chamber. Each  $\pi^0$  produced at the interaction vertex decays to two  $\gamma$ 's and about  $2/10$  of these  $\gamma$ 's will produce an electron pair in the exit window ( $\sim .3$  rad. length thick). These will produce extra tracks downstream which did not originate at the production vertex. We draw the following conclusions from a Monte Carlo simulation of this problem:

- i.) For  $E\gamma >$  a few GeV, most of the produced electrons enter the downstream counters. From the downstream information alone, these will be indistinguishable from tracks originating

at the interaction vertex. However, they will not match up with any track which can be resolved in the bubble chamber. Hence, it is unlikely that these tracks will preclude particle counting and single-particle momentum studies on an event-by-event basis except in those events in which an unresolved forward jet of particles appears in the bubble chamber. For such events, the effects of conversion electrons can be removed on a statistical basis.

- ii.) For  $E_\gamma \gtrsim 10$  GeV, a significant fraction of the produced pairs can, in principle, be reconstructed; i. e., both  $e^+$  and  $e^-$  traverse the first 3 downstream chambers. Hence, it is likely that these conversion electrons can be used to advantage in estimating  $\pi^0$  production. As a further estimate of the  $\pi^0$  production, one can place! [ during a short part of each run ] a centimeter of lead in front of the second downstream chamber and convert the major portion of  $\gamma$  rays. This will yield a good estimate of the  $\pi^0$  production.

### APPENDIX III

#### Three Constraint Fits

We have used a Monte Carlo technique to determine whether the elastic events and those events where the target proton dissociates into all charged particles, can be separated from those events in which an additional  $\pi^0$  is produced. The only information on the fast outgoing particle is its position and angle in space and we therefore have what would be, in standard terminology, a three constraint fit.

In order to determine the accuracy needed in the angle determination for this fit to give a clean separation, the following method has been used:

First, the Monte Carlo program NVERTX was used to generate a sample of elastic events and also a sample of events in which an additional low momentum  $\pi^0$  was produced. In both cases it was assumed that the momentum transfer from the beam to the fast secondary had a distribution of the form  $e^{-7.5 t}$ . For the case where the  $\pi^0$  was produced, it was assumed that the target proton and the  $\pi^0$  formed a low mass system of between 1200 and 1700 MeV invariant mass. This is the shape seen at lower energies and considered as the dissociation of the target proton. This system was then allowed to decay isotropically in its rest frame.

In each case, then, the angle and momentum of the slow particle were given gaussian errors to simulate measurements in the chamber. The errors have been set to .01 radians in angle and 1% in momentum. These are reasonable errors, based upon our experience with this chamber, for any proton with a momentum of  $\sim 225$  MeV/c or greater. These calculations, therefore, are valid for  $|t| \geq 0.05$  GeV/c for elastic scattering. Below that, these errors should be set larger and the possible contamination would rise.

Using these perturbed values, then, and a good knowledge of the beam momentum and direction from the upstream system, a prediction is made of the angle in the laboratory at which the fast particle should come off if the event were elastic. In figure 1 of this appendix we have plotted the difference between the prediction and the particle's real angle for the two different cases. If we define as elastic any particle which has an angle within  $\pm 0.05$  mr of the elastic prediction, then there is a 7% misidentification with the  $\pi^0$  events assuming equal cross sections. Since there are two independent angles which are predicted (azimuth and dip) the overall contamination is reduced to  $< 0.5\%$ .

If we therefore place an additional set of planes, identical to those described in Appendix II, at a distance of 30 meters from the chamber, then our cut corresponds to  $\pm 3$  wires. The angle subtended by this plane of  $\pm 5$  mr corresponds to a momentum transfer of about  $6(\text{GeV}/c)^2$  at 500 GeV so there is no practical restriction on the  $t$  range.

This analysis has also been carried out when the proton dissociates into  $(P\pi^+\pi^-)$ . The contamination of this state with  $(P\pi^+\pi^-\pi^0)$ , assuming equal cross section, is  $\sim 3\%$ .

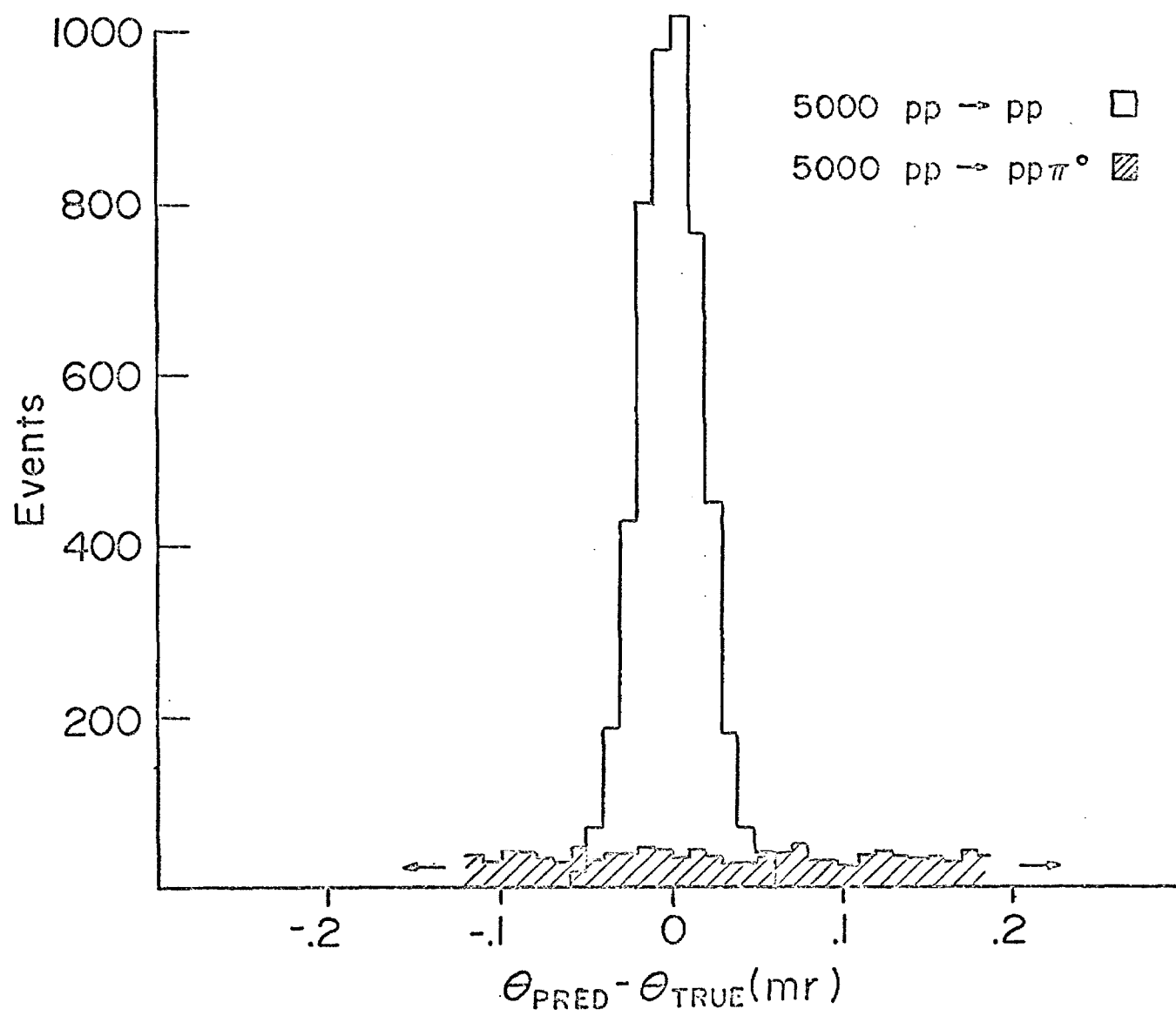
Another source of contamination is when the beam dissociates into, in the simplest case,  $(\text{beam} + \pi^0)$ . We have studied this case also and find that the contamination depends somewhat on the decay distribution of the dissociating particle. For a proton beam going into  $P\pi^0$ , where we expect a relatively isotropic distribution, there is virtually no contamination ( $< 1\%$ ). If we consider a meson beam which dissociates into  $(\pi^\pm\pi^0)$  and assume a decay distribution of  $\cos^2\theta$  with respect to production angle of the 'heavy' pion then we get a contamination of  $\sim 1\%$ . The dissociation into three pions should contribute almost no contamination.

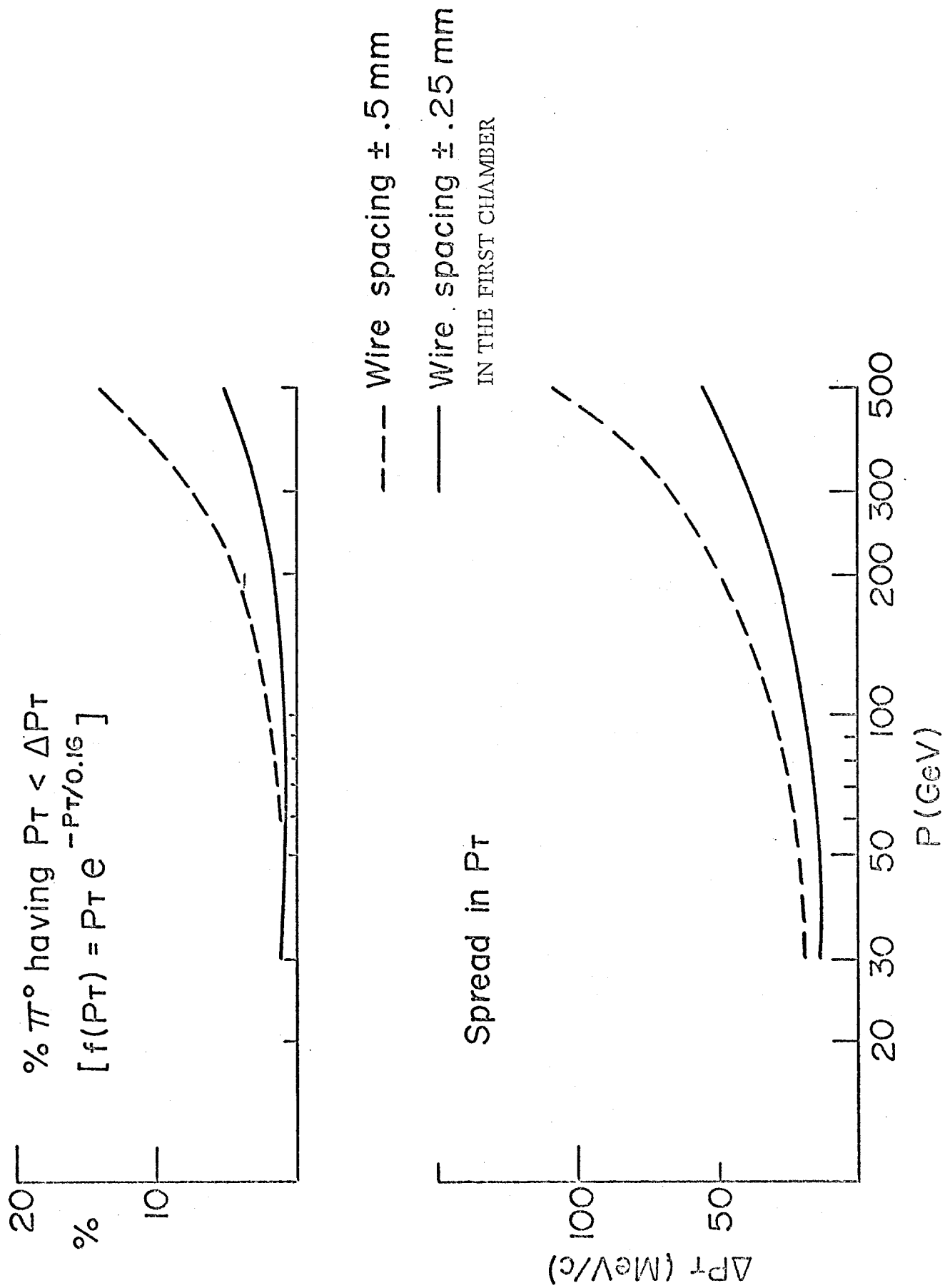


Another way of looking at this method of separating out three constraint fits is that we have a certain resolution in our determination of the transverse momentum present in the interaction. It is clear, then, that we can separate out any event in which a  $\pi^0$  carries off more than this minimum transverse momentum. If we consider then the measurement of the fast outgoing track, we get a minimum resolvable transverse momentum which is shown in Fig. 2 of the appendix. Assuming, then, a transverse momentum distribution for the  $\pi^0$ 's given by

$$f(P_t) = P_t e^{-P_t/0.16}$$

then the number of events for which the transverse momentum is less than the resolvable momentum is given in the upper half of the figure. For 0.5mm wire spacing this contamination is  $\sim 5\%$  at 500 GeV. This method, which depends upon measuring the fast outgoing particle, is not as powerful as the one previously described, which uses only the well measured particles to predict the final position of the fast outgoing track. However, this less powerful technique gives a lower limit to our ability to separate the elastic scattering. It should be emphasized that the above estimates assume equal cross sections for the two reactions; however, we expect that the contaminate cross section should be only a fraction of the elastic cross section and hence the percentage confusion quoted above will be reduced by this fraction.





## APPENDIX IV

## Measurement of Invariant Masses

On page 2 of this appendix there is a calculation which shows how the errors in the angles and momentum measurements for two outgoing particles effect the calculation of the invariant mass. This has been checked by using the Monte Carlo as has been discussed in Appendix I. The only change has been to first throw a "resonance" with the same distribution of transverse momentum as was discussed in Appendix I and then allow the resonance to decay isotropically in its rest frame. After transforming to the laboratory system, the same swimming as has been presiously discussed was carried out on all particles which went through the counters. For the particles which did not make it into the downstream system errors of 0.01 radians in angle and 1% in momentum have been assumed.

In the figure on page 3 of this appendix we show the results of this Monte Carlo for resonances of 500, 1000, and 1500 MeV invariant mass and for the various momenta. The results are quite good, generally  $< 5\%$  for momentum up to 100 GeV/c, when both particles go into the system (solid line). The results are considerably worse when one or both are not in the downstream chambers. This is probably because the error in the angle gets large compared with the opening angle between the two particles.

At 20 GeV, only 5% of the events have both particles in the system. By 100 GeV the situation is quite different. For the 500 MeV particles, almost 95% are now completely in the downstream system while for the 1000 MeV and 1500 MeV particles, these percentages are 80% and 75% respectively. These latter percentages are lower than the case of the 500 MeV particle because of the higher  $Q$  value of these resonances together with the assumption of isotropic decay. For the more realistic case where these higher mass objects have spin and decay anisotropically (for example like  $\cos^2 \theta$ ) these percentages would be higher.

Error analysis of measured invariant mass.

$$M^2 = (\sum E_i)^2 - (\sum \vec{p}_i)^2 = \sum E_i^2 - \sum p_i^2 + \sum_{i \neq j} E_i E_j - p_i p_j \cos \theta_{ij}$$

$$= + \sum M_i^2 + \sum_{i \neq j} E_i E_j - p_i p_j \cos \theta_{ij}$$

$$\delta(M^2) = \sum_{i \neq j} p_i \frac{E_j}{E_i} \delta p_i + p_j \frac{E_i}{E_j} \delta p_j - p_j \cos \theta_{ij} \delta p_i - p_i \cos \theta_{ij} \delta p_j$$

$$+ p_i p_j \sin \theta_{ij} \delta \theta_{ij}$$

$$= \sum_{i \neq j} \left( p_i \frac{E_j}{E_i} - p_j \cos \theta_{ij} \right) \delta p_i + \left( p_j \frac{E_i}{E_j} - p_i \cos \theta_{ij} \right) \delta p_j$$

$$+ p_i p_j \sin \theta_{ij} \delta \theta_{ij}$$

$$[\delta(M^2)]^2 = \sum_{i \neq j} \left( p_i \frac{E_j}{E_i} - p_j \cos \theta_{ij} \right)^2 (\delta p_i)^2 + \left( p_j \frac{E_i}{E_j} - p_i \cos \theta_{ij} \right)^2 (\delta p_j)^2$$

$$+ (p_i p_j \sin \theta_{ij})^2 (\delta \theta_{ij})^2$$

For  $p \sim E$  and  $\theta_{ij}$  small ( $\cos \theta \sim 1 - \frac{\theta^2}{2}$ ,  $\sin \theta \sim \theta$ )

$$[\delta(M^2)]^2 \sim \sum_{i \neq j} \left( \frac{p_j \theta_{ij}^2}{2} \right)^2 (\delta p_i)^2 + \left( \frac{p_i \theta_{ij}^2}{2} \right)^2 (\delta p_j)^2 + (p_i p_j \theta_{ij})^2 (\delta \theta_{ij})^2$$

$$\sim \sum_{i \neq j} \left( \frac{p_i p_j \theta_{ij}^2}{2} \right)^2 \left[ \left( \frac{\delta p_i}{p_i} \right)^2 + \left( \frac{\delta p_j}{p_j} \right)^2 + 4 \left( \frac{\delta \theta_{ij}}{\theta_{ij}} \right)^2 \right]$$

$$M^2 \sim \sum_{i \neq j} \frac{p_i p_j \theta_{ij}^2}{2} \quad ; \quad \frac{\delta M^2_{rms}}{M^2} \sim \sqrt{\frac{\sum_{i \neq j} \left( \frac{p_i p_j \theta_{ij}^2}{2} \right)^2 \left[ \left( \frac{\delta p_i}{p_i} \right)^2 + \left( \frac{\delta p_j}{p_j} \right)^2 + 4 \left( \frac{\delta \theta_{ij}}{\theta_{ij}} \right)^2 \right]}{\sum_{i \neq j} \frac{p_i p_j \theta_{ij}^2}{2}}}$$

For 2-body case:  $\frac{\delta M^2_{rms}}{M^2} \sim \left[ \left( \frac{\delta p_1}{p_1} \right)^2 + \left( \frac{\delta p_2}{p_2} \right)^2 + 4 \left( \frac{\delta \theta_{12}}{\theta_{12}} \right)^2 \right]^{1/2}$

